Partial array imaging in acoustic waveguides

Chrysoula Tsogka

Work in collaboration with D. Mitsoudis and S. Papadimitropoulos

University of Crete and IACM-FORTH
currently Visiting Professor at Stanford University

BIRS January 17-22, 2016

Table of contents

Table of contents

Problem description

Goal : Imaging extended scatterers in the sea using acoustic waves.

Marine model environment : 2D, homogeneous waveguide with horizontal pressure release bdries, constant sound speed c_0 and density ρ.

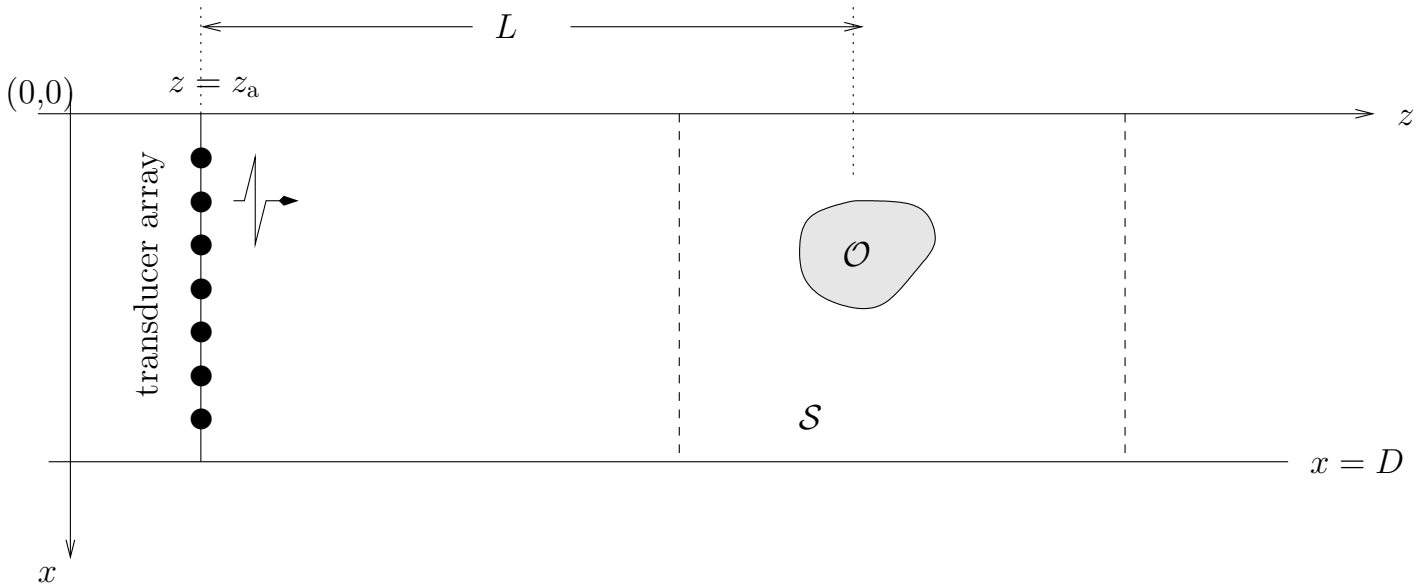

$\mathcal{O}$: extended scatterer (typical size $\sim$ wavelength, λ_0).
D : depth, $D \gg \lambda_0$
L : range (distance between array and scatterer), $L \gg D$

Array imaging setup

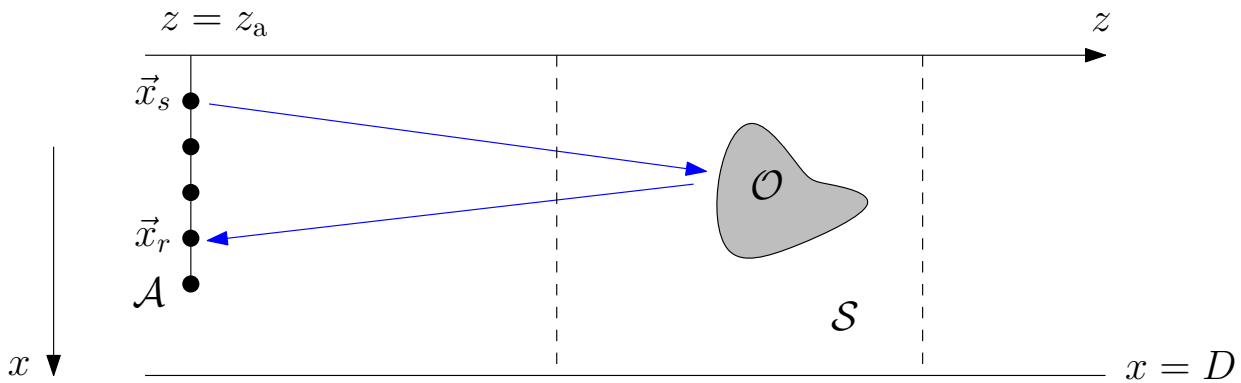

- vertical array $\mathcal{A}$: N equidistant transducers (h : inter-element distance).
  - $\mathcal{A} = [0, D]$: full array.
  - $\mathcal{A} \subset [0, D]$: partial array.
- Array response matrix $\hat{\Pi}(\omega) \in \mathbb{C}^{N \times N}$: $[\hat{\Pi}(\omega)]_{rs}$ = the Fourier transform of the time traces recorded at the r-th transducer due to a δ–function impulse generated by the s-th transducer, for a given frequency ω.
- Data : Array response matrix for the scattered field.
- $\mathcal{S}$: search domain.

Notation

$\hat{G}(\vec{\boldsymbol{x}}, \vec{\boldsymbol{x}}_{\rm s})$ outgoing Green's function for the Helmholtz operator $-\Delta \cdot -k^2 \cdot$

$$\hat{G}(\vec{\boldsymbol{x}}, \vec{\boldsymbol{x}}_{\rm s}) = \frac{\mathrm{i}}{2} \sum_{n=1}^{\infty} \frac{1}{\beta_n} \mathrm{e}^{\mathrm{i}\,\beta_n |z - z_{\rm s}|} X_n(x) X_n(x_{\rm s}),$$

where k is the (real) wavenumber and $\{\mu_n, X_n\}_{n=1,2,\ldots}$ eigenpairs of

$$X''(x) + \mu X(x) = 0, \ x \in (0, D) \quad \text{and} \quad X(0) = X(D) = 0,$$

i.e.,

$$\mu_n = (n\pi/D)^2, \quad X_n(x) = \sqrt{2/D} \sin(\sqrt{\mu_n} x), \ n = 1, 2, \ldots.$$

Assume $\exists$ an index M s.t.

$$\mu_M < k^2 < \mu_{M+1},$$

horizontal wavenumbers : $\beta_n = \begin{cases} \sqrt{k^2 - \mu_n}, & 1 \le n \le M, \quad \rightsquigarrow \text{ propagating modes} \\ \mathrm{i}\sqrt{\mu_n - k^2}, & n \ge M+1, \quad \rightsquigarrow \text{ evanescent modes} \end{cases}$

Table of contents

Kirchhoff migration (KM) functional

At frequency ω and for a search point $\vec{\boldsymbol{y}}^{\,\mathrm{s}} = (z^{\mathrm{s}}, x^{\mathrm{s}}) \in \mathcal{S}$

$$\mathcal{I}^{\mathrm{KM}}(\vec{\boldsymbol{y}}^{\,\mathrm{s}}, \omega) = \sum_{r=1}^{N} \sum_{s=1}^{N} \overline{\hat{G}(\vec{\boldsymbol{x}}_r, \vec{\boldsymbol{y}}^{\,\mathrm{s}}, \omega)} \hat{\Pi}(\vec{\boldsymbol{x}}_r, \vec{\boldsymbol{x}}_s, \omega) \, \overline{\hat{G}(\vec{\boldsymbol{x}}_s, \vec{\boldsymbol{y}}^{\,\mathrm{s}}, \omega)},$$

where $\vec{\boldsymbol{x}}_r = (z_{\mathrm{a}}, x_r)$, $\vec{\boldsymbol{x}}_s = (z_{\mathrm{a}}, x_s)$.

Remark that this can be used either for full or partial array aperture.

Alternative imaging functional - Modal Projection

$\mathcal{A} = [0, D]$: full array.

Introduce a weighted modal projection of the array response matrix, *i.e.*, a matrix $\hat{\mathbb{P}}(\omega)$, such that $\forall m, n = 1, 2, \ldots, M$,

$$\underbrace{\hat{\mathbb{P}}_{mn}(\omega)}_{M \times M} = \beta_m \beta_n \int_0^D \int_0^D \underbrace{\hat{\Pi}(\vec{x}_s, \vec{x}_r, \omega)}_{N \times N} X_m(x_s) X_n(x_r) \, dx_r \, dx_s,$$

or, in matrix form,

$$\hat{\mathbb{P}} = h^2 \, D_\beta^{-1} \, V^T \, \hat{\Pi} \, V \, D_\beta^{-1},$$

where $D_\beta = \mathrm{diag}(\frac{1}{\beta_1}, \ldots, \frac{1}{\beta_M})$, and $V_{k\ell} = X_\ell(x_k)$, $k = 1, \ldots, N$, $\ell = 1, \ldots, M$.

Define the imaging functional

$$\widetilde{\mathcal{I}}^{\mathrm{KM}}(\vec{\boldsymbol{y}}^{\,\mathrm{s}},\omega) = -\frac{1}{4h^2}\sum_{m,n=1}^{M} \mathrm{e}^{-\mathrm{i}\,(\beta_n+\beta_m)|z_{\mathrm{a}}-z^{\mathrm{s}}|}\, X_n(x^{\mathrm{s}})X_m(x^{\mathrm{s}})\,\hat{\mathbb{P}}_{mn}(\omega).$$

Table of contents

Selective imaging (free space)

Goal : Imaging specific parts of the scatterer.

We follow the subspace projection method
Borcea, Papanicolaou, Guevara–Vasquez, *SIAM J. Imaging Sci.*, 2008.

Motivated by selective focusing of multiple 'point' scatterers. DORT method.
Prada, Fink, *Wave Motion*, 1994.
Hazard, Ramdani, *SIAM J. Appl. Math.*, 2004.
Pinçon, Ramdani, *IP*, 2007.

Based on the SVD of the array response matrix

$$\hat{\Pi}(\omega) = U(\omega)\Sigma(\omega)V^*(\omega) = \sum_{i=1}^{N} \sigma_i(\omega)U_i(\omega)V_i^*(\omega),$$

where

- Σ : a diagonal matrix containing the singular values σ_i,
- U, V : unitary matrices containing the left & right singular vectors, resp.

Selective imaging in waveguides

We create a filtered version of $\hat{\mathbb{P}}(\omega)$,

$$D[\hat{\mathbb{P}}(\omega)] = \sum_{i=1}^{M} d_i \sigma_i U_i V_i^*, \text{ where the filter weights } d_i = 0 \text{ or } 1.$$

To create selective focusing images use

$$\widetilde{\mathcal{I}}^{\mathrm{KM,f}}(\vec{\boldsymbol{y}}^{\,\mathrm{s}}, \omega) = -\frac{1}{4h^2} \sum_{m,n=1}^{M} \mathrm{e}^{-\mathrm{i}\,(\beta_n+\beta_m)|z_{\mathrm{a}}-z^{\mathrm{s}}|} X_n(x^{\mathrm{s}}) X_m(x^{\mathrm{s}}) \Big(D[\widehat{\mathbb{P}}(\omega)] \Big)_{mn}.$$

$$\widetilde{\mathcal{I}}_J^{\mathrm{KM}}(\vec{\boldsymbol{y}}^{\,\mathrm{s}}, \omega) = -\frac{1}{4h^2} \sum_{m,n=1}^{M} \mathrm{e}^{-\mathrm{i}\,(\beta_n+\beta_m)|z_{\mathrm{a}}-z^{\mathrm{s}}|} X_n(x^{\mathrm{s}}) X_m(x^{\mathrm{s}}) \Big(\sigma_J(\omega) U_J(\omega) V_J^*(\omega) \Big)_{mn}.$$

Table of contents

A model problem - full array

1d vertical reflector ('crack') $\mathcal{T}$ of width b, centered at (L, x_0)

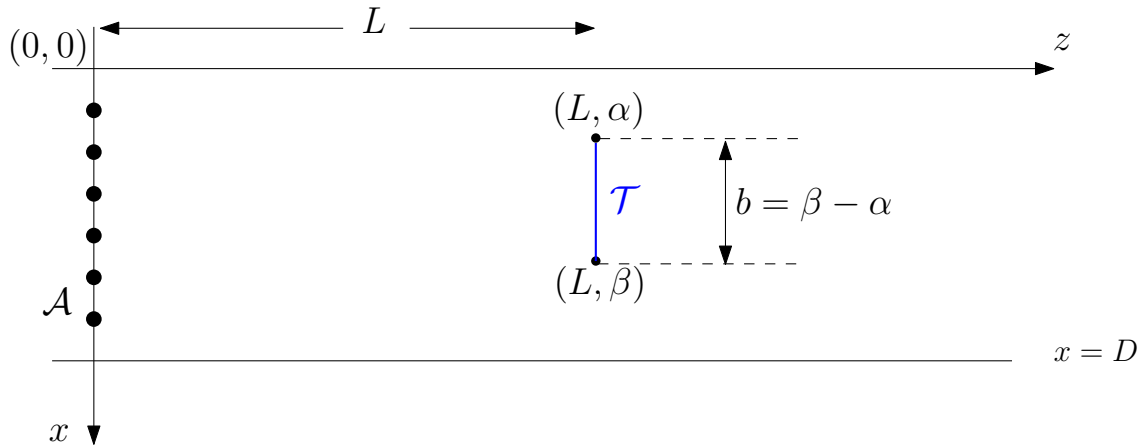

Receiver $\vec{\boldsymbol{x}}_r = (0, x_r)$, source $\vec{\boldsymbol{x}}_s = (0, x_s)$, $r, s \in \{1, 2, \ldots, N\}$

$$\hat{\Pi}(\vec{x}_r; \vec{x}_s, \omega) = k^2 \int_{\mathcal{T}} \hat{G}(\vec{\boldsymbol{y}}, \vec{\boldsymbol{x}}_r)\hat{G}(\vec{\boldsymbol{y}}, \vec{\boldsymbol{x}}_s)\, dx, \quad \text{array response matrix} \quad \left(\vec{\boldsymbol{y}} = (L, x)\right)$$

(assuming unit reflectivity for the target.)

inserting $\hat{G}$ ...

$$\hat{\Pi}(\vec{x}_r;\vec{x}_s,\omega) = -\frac{1}{4}\sum_{m,n=1}^{\infty} \frac{e^{i\beta_m L}}{\beta_m} X_m(x_s) \frac{e^{i\beta_n L}}{\beta_n} X_n(x_r) \int_{\mathcal{T}} X_m(x) X_n(x) dx,$$

$$\beta_n = \begin{cases} \sqrt{k^2-\mu_n}, & n=1,\ldots,M \\ i\sqrt{\mu_n-k^2}, & n\geq M+1 \end{cases}, \qquad \mu_n = \left(\tfrac{n\pi}{D}\right)^2, \qquad X_n = \sqrt{\tfrac{2}{D}} \sin\sqrt{\mu_n}x, \qquad n=1,2,\ldots$$

In matrix form

$$\hat{\Pi} = \mathcal{G}\, A_{\text{inf}}\, \mathcal{G}^T$$

where

$$\mathcal{G}_{k\ell} = g_\ell(x_k) := \frac{i}{2}\frac{\mathrm{e}^{\mathrm{i}\,\beta_\ell L}}{\beta_\ell} X_\ell(x_k) = \left(\hat{G}(\cdot,\vec{\boldsymbol{x}}_k), X_\ell\right)_{L^2[0,D]}$$

$\ell = 1,2,\ldots, \quad k = 1,2,\ldots,N.$

Remark

$\mathcal{G}_{k\ell} \approx 0$ for $\ell \geq M+1$ $\therefore$ A_M (the $M \times M$ principal submatrix of A_{inf}) is relevant

On the other hand,

$$\widehat{\mathbb{P}} = -\frac{1}{4} Q\, A_M\, Q, \quad Q = \mathrm{diag}(\mathrm{e}^{\mathrm{i}\,\beta_1 L}, \ldots, \mathrm{e}^{\mathrm{i}\,\beta_M L})$$

$\therefore \widehat{\mathbb{P}}$ is unitarily equivalent to A_M, since $Q^* Q = I$.

On the other hand,

$$\widehat{\mathbb{P}} = -\frac{1}{4} Q\, A_M\, Q, \quad Q = \mathrm{diag}(\mathrm{e}^{\mathrm{i}\,\beta_1 L}, \ldots, \mathrm{e}^{\mathrm{i}\,\beta_M L})$$

$\therefore \widehat{\mathbb{P}}$ is unitarily equivalent to A_M, since $Q^* Q = I$.

Need to explore the spectral properties of A_M

Spectral properties of the $n \times n$ matrix A_n

$$
\begin{aligned}
a_{\ell m} &= \int_\alpha^\beta X_\ell(x) X_m(x) dx \\
&= \frac{1}{D}\int_\alpha^\beta \cos\frac{(\ell-m)\pi x}{D} dx - \frac{1}{D}\int_\alpha^\beta \cos\frac{(\ell+m)\pi x}{D} dx.
\end{aligned}
$$

$$
\therefore \quad A_n = T_n - H_n,
$$

where

$T_n := (t_{\ell-m})_{\ell,m=1}^n$ Toeplitz $\qquad H_n := (t_{\ell+m})_{\ell,m=1}^n$ Hankel

and

$$
t_m = \frac{1}{D}\int_0^D \mathbb{1}_{\mathcal{T}}(x) \cos\frac{m\pi x}{D} dx, \quad m = 1, 2, \ldots
$$

$\mathbb{1}_{\mathcal{T}}(x)$: generating function of T_n and H_n

Proposition

Let $\nu_1^{(n)} \leq \nu_2^{(n)} \leq \ldots \leq \nu_n^{(n)}$ *eigenvalues of* A_n.

- $0 \leq \nu_i^{(n)} \leq 1$, *for all* $i = 1, \ldots, n$,
- *for any fixed integer* k, $\nu_k^{(n)} \to 0$, $\nu_{n-k}^{(n)} \to 1$, *as* $n \to \infty$,
- $\lim_{n\to\infty} \frac{1}{n}\Big(\#\{k:\ \nu_k^{(n)} \in (\epsilon, 1-\epsilon) \ \ \textit{for } \epsilon > 0\}\Big) = 0$, *and*
- $\lim_{n\to\infty} \frac{1}{n}\sum_{i=1}^{n} \nu_i^{(n)} = \frac{1}{D}\int_0^D \mathbb{1}\tau(x)\,dx = \frac{b}{D} \rightsquigarrow$ ratio of non-zero eigs to total

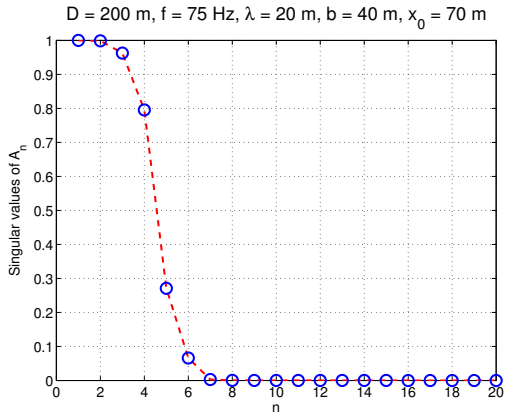

$n = 20$

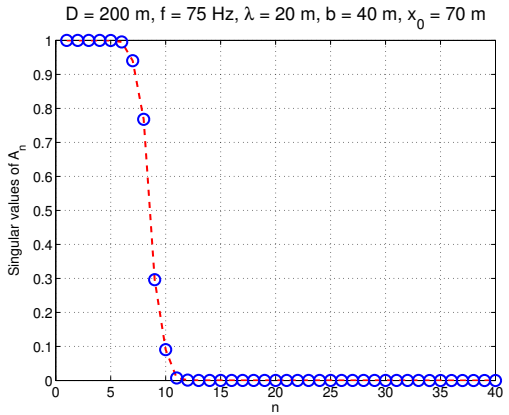

$n = 40$

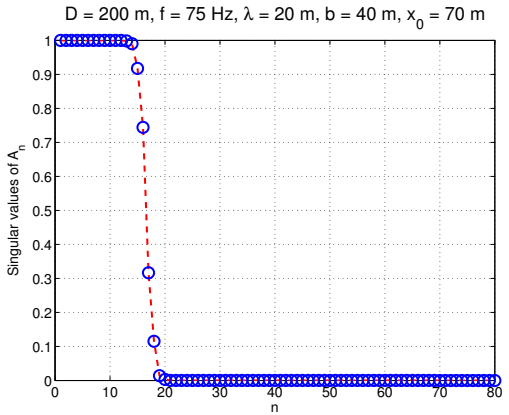

$n = 80$

– Grenander & Szegő, *Toeplitz Forms and their Applications*, 1984

– Trench, Asymptotic distribution of the even and odd spectra of real symmetric Toeplitz matrices, *Linear Algebra Appl.*, 1999

Number of 'significant' singular values for A_M

In our case $n = M$ (= number of propagating modes)

$\therefore$ the number of 'significant' singular values for A_M is expected to be roughly

$$\left[M\,\frac{b}{D}\right] \approx \left[\frac{b}{\lambda/2}\right]$$

size of the scatterer devided by the array resolution (as in free space)

E.g. $f = 75.5$ Hz, $D = 200$ m, $c_0 = 1500$ m/s, $\lambda = 19.87$ m, $M = 20$.

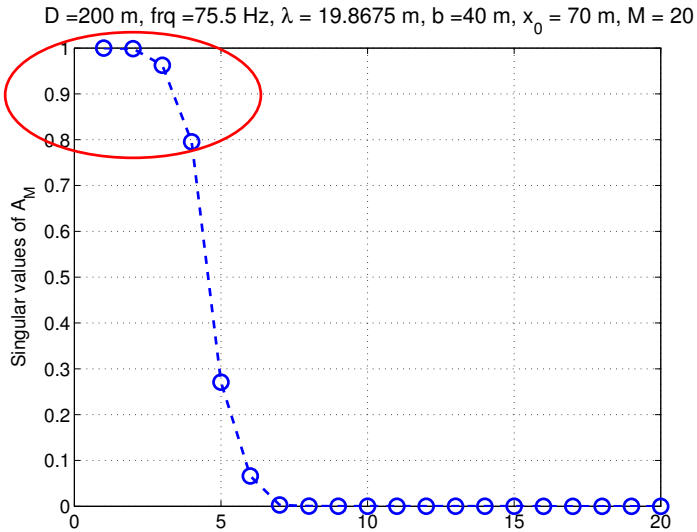

$b = 40$ m $\approx 2\lambda \rightsquigarrow$ 4 significant s.v.'s

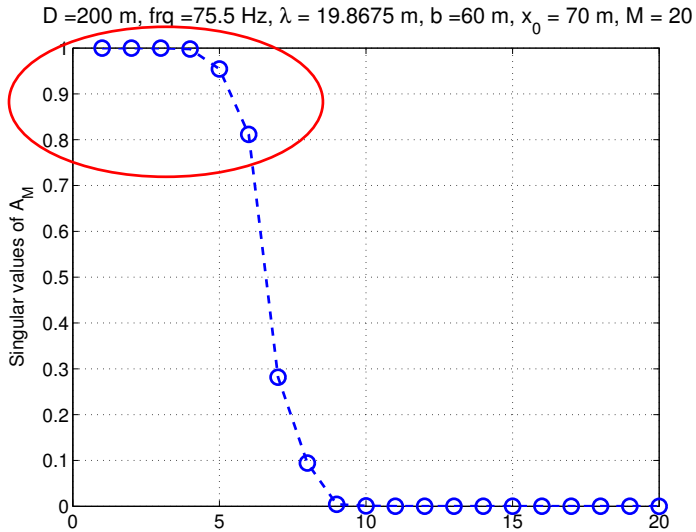

$b = 60$ m $\approx 3\lambda \rightsquigarrow$ 6 significant s.v.'s

Selective imaging

Consider $\widetilde{\mathcal{I}}_J^{\mathrm{KM}}$ for a search point $\vec{\boldsymbol{y}}^{\,\mathrm{s}} = (L, x^{\mathrm{s}})$ **located at the correct range** L.

$$\widetilde{\mathcal{I}}_J^{\mathrm{KM}}(\vec{\boldsymbol{y}}^{\,\mathrm{s}}) = \frac{1}{16h^2} \sum_{m,n=1}^{M} X_m(x^{\mathrm{s}}) X_n(x^{\mathrm{s}}) (\sigma_J u_m^J u_n^J) = \sigma_J \left(\frac{1}{4h} \sum_{n=1}^{M} u_n^J X_n(x^{\mathrm{s}}) \right)^2,$$

where

$$\boldsymbol{u}^J = (u_1^J, u_2^J, \ldots, u_M^J)^T \text{ is the s.vec. of } A_M \rightsquigarrow \text{ the s.val. } \sigma_J.$$

Natural to associate to $\boldsymbol{u}^J$ the trig. polynomial

$$s_J(x) = \sum_{n=1}^{M} u_n^J \sin \frac{n\pi x}{D}$$

and explore its properties for various J.

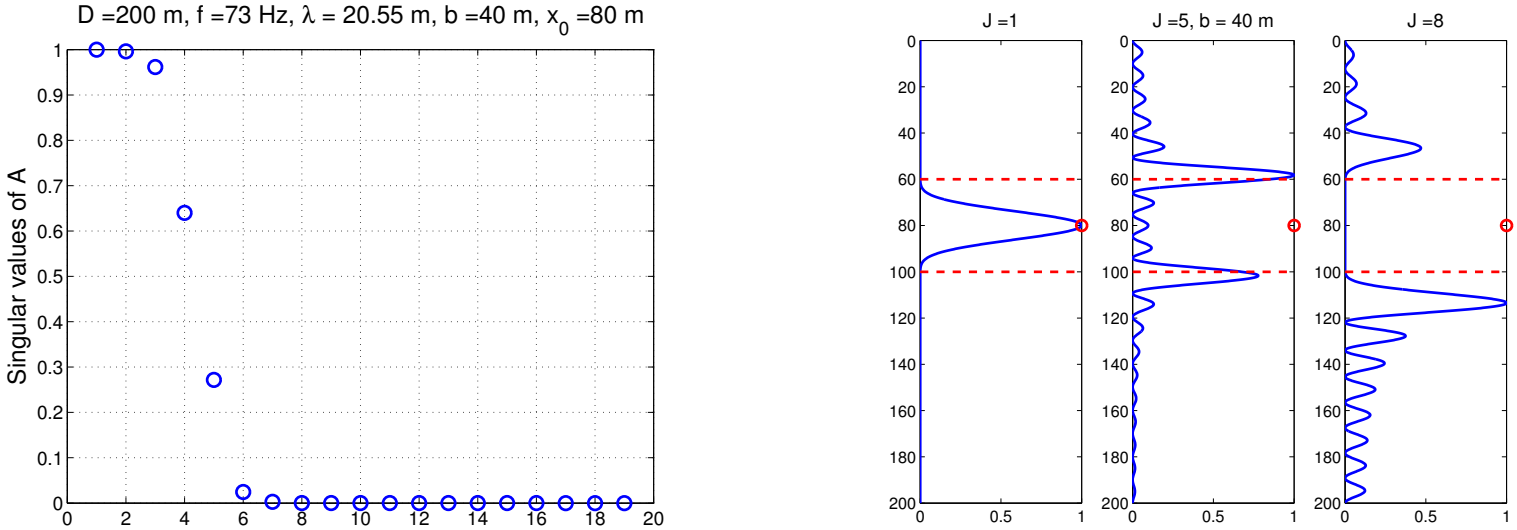

Figure : Left : The singular values of A_M $(M = 19)$. Right : The normalized graphs of $(s_J(x))^2$, $x \in [0, 200]$, for $J = 1, 5, 8$

$J = 1 \rightsquigarrow$ signal subsp.
$J = 5 \rightsquigarrow$ transient subsp.
$J = 8 \rightsquigarrow$ noise subsp.

Slepian, Prolate spheroidal wave functions, 1978
Hanke, Nagy, Inverse Toeplitz preconditioners for ill-posed problems, 1998

Easy to show that

$$\frac{\|s_J\|^2_{L^2[\alpha,\beta]}}{\|s_J\|^2_{L^2[0,D]}} = \sigma_J.$$

Therefore the trigonometric polynomial that corresponds to the first singular vector $\boldsymbol{u}^1$ and, consequently, the associated image computed at the correct range L, exhibit the largest fractional concentration of energy in (α, β).

Easy to show that

$$\frac{\|s_J\|^2_{L^2[\alpha,\beta]}}{\|s_J\|^2_{L^2[0,D]}} = \sigma_J.$$

Therefore the trigonometric polynomial that corresponds to the first singular vector $\boldsymbol{u}^1$ and, consequently, the associated image computed at the correct range L, exhibit the largest fractional concentration of energy in (α, β).

What about the eigenvectors of the matrix A_M ?

Try to characterise them depending on the various positions of the crack.

A crack attached on the top of the waveguide

In this case the eigenvectors of the matrix A_M may be recovered by the skew-symmetric ($u^J_{-i} = -u^J_i$, $i = 1, \ldots, M$) eigenvectors of the matrix T_{2M+1} which satisfy

$$\sum_{n=-M}^{M} \frac{1}{(m-n)\pi} \sin\frac{(m-n)\pi b}{D} u^J_n = \nu_J u^J_m, \quad m = -M, \ldots, M$$

$\therefore \{u^J_i\}_{i=-M}^{M}$ is a *discrete prolate spheroidal sequence (DPSS) or Slepian sequence*, a discrete analog of the *prolate spheroidal wave function (PSWF)* ψ_{2J-1}.

Recall, ψ_n is the eigenfunction $\rightsquigarrow$ the n-th eigenvalue of the Fredholm integral equation

$$\int_{-1}^{1} \frac{\sin c(x-y)}{\pi(x-y)} \psi_n(y)\, dy = \mu_n \psi_n(x), \quad x \in [-1, 1],$$

Here, the bandwidth parameter : $c = \frac{2\pi b}{\lambda} = bk$, where k is the wavenumber.

Moreover, we can show that

$$s_J(x) \approx \text{Const.}\, \psi_{2J-1}\left(\frac{x}{b}\right), \quad x \in [0, D].$$

The graph of $(s_J(x))^2$ vs. the graph of $\left(\psi_{2J-1}\left(\frac{x}{b}\right)\right)^2$, for $x \in [0, 200]$.
$f = 73$ Hz, $b = 40$ m.

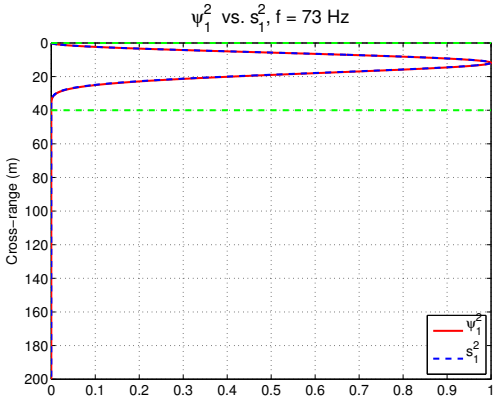

$J = 1$

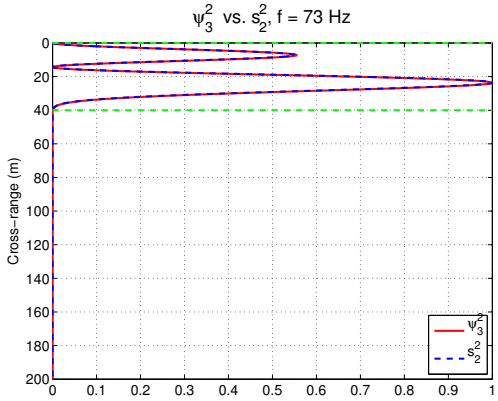

$J = 2$

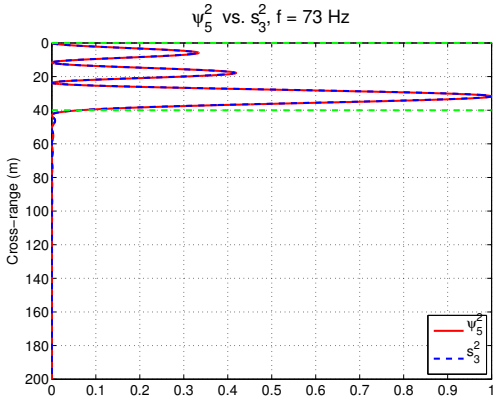

$J = 3$

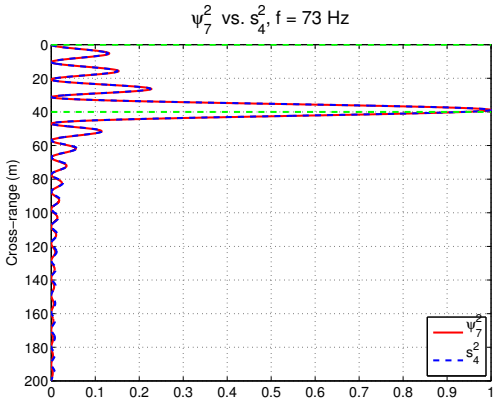

$J = 4$

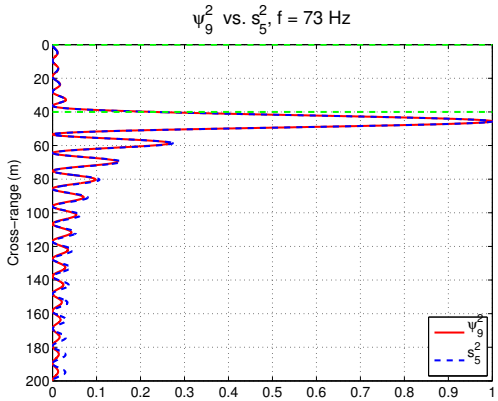

$J = 5$

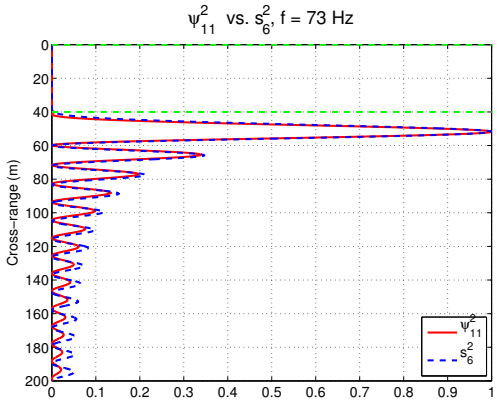

$J = 6$

A crack attached on the bottom of the waveguide

Easy to show that

$$s_J^{\text{bot}}(x) = s_J^{\text{top}}(D - x),$$

$\therefore$ the image created by the imaging functional $\widetilde{\mathcal{I}}_J^{\text{KM}}$, at the correct range L, is determined by the graph of the PSWF $\left(\psi_{2J-1}\left(\frac{D-x}{b}\right)\right)^2$, $x \in [0, D]$.

A crack located in the interior of the waveguide

The eigenvectors of A_M are determined through the skew-symmetric eigenvectors of the matrix T_{2M+1}, where they now satisfy

$$\sum_{n=-M}^{M} \frac{1}{(m-n)\pi} \left(\sin \frac{(m-n)\pi\beta}{D} - \sin \frac{(m-n)\pi\alpha}{D} \right) u_n^J = \nu_J u_m^J,$$

for $m = -M, \ldots, M$.

This is the discrete analog of the integral equation

$$K_1 u(x) := \int_{-1}^{1} \frac{1}{(x-y)\pi} \left(\sin k\beta(x-y) - \sin k\alpha(x-y) \right) u(y)\, dy = \nu u(x),$$

for $x \in [-1, 1]$.

K_1 is a compact symmetric operator from $L^2[-1,1]$ to $L^2[-1,1]$, hence its eigenvalues $\nu_0 \geq \nu_1 \geq \cdots \geq \nu_n \geq \cdots \to 0$, as $n \to \infty$, while its corresponding eigenfunctions are complete in $L^2[-1,1]$.

Moreover, we may show that

$$s_J(x) \approx \text{Const.}\, v(x), \quad x \in [0, D],$$

where v is an odd σ_J–eigenfunction of the integral equation

$$K_2 v(x) := \int_{\mathcal{J}} \frac{\sin k(x-y)}{\pi\,(x-y)}\, v(y)\, dy = \nu v(x), \quad x \in \mathcal{J} := [-\beta, -\alpha] \cup [\alpha, \beta],$$

Note that $\mathcal{J}$ is a disconnected interval, while the kernel is a sinc function with bandwidth parameter equal to the wavenumber.

K_2 is also a compact symmetric operator from $L^2(\mathcal{J})$ to $L^2(\mathcal{J})$, that has the same eigenvalues with K_1, and its corresponding eigenfunctions are complete in $L^2(\mathcal{J})$.

SenGupta et al., *J. Fourier Anal. Appl.*, 2012

The graph of $(s_J(x))^2$ vs. the graph of $v^2(x)$, for $x \in [0, 200]$.
$f = 73$ Hz, $\alpha = 60$ m and $\beta = 100$ m, $(b = 40$ m$)$.

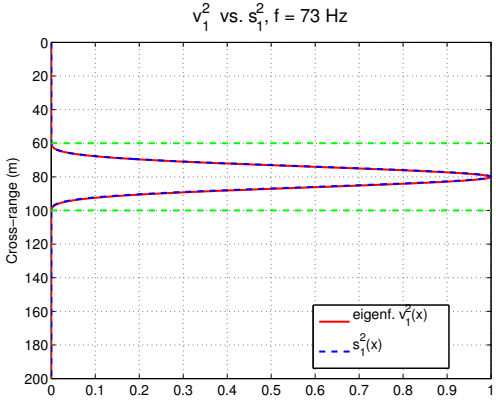

$J = 1$

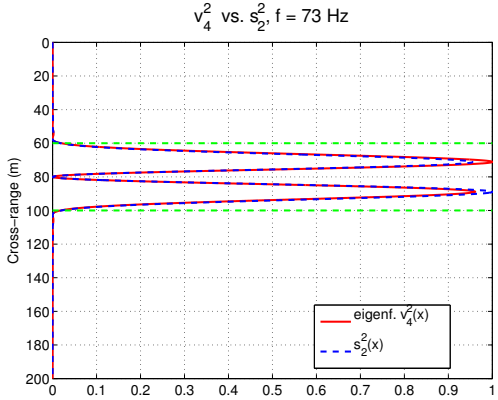

$J = 2$

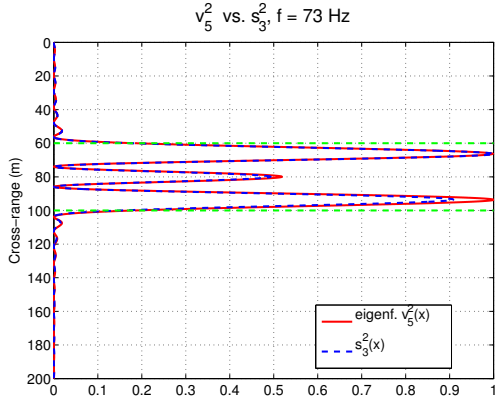

$J = 3$

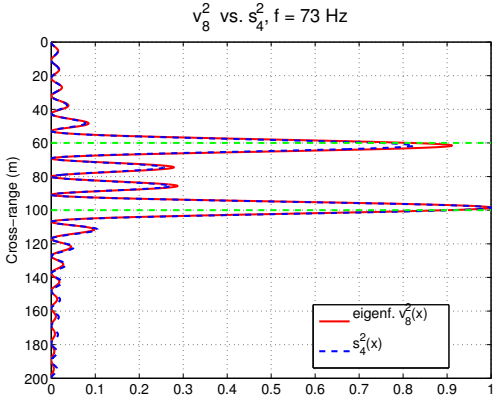

$J = 4$

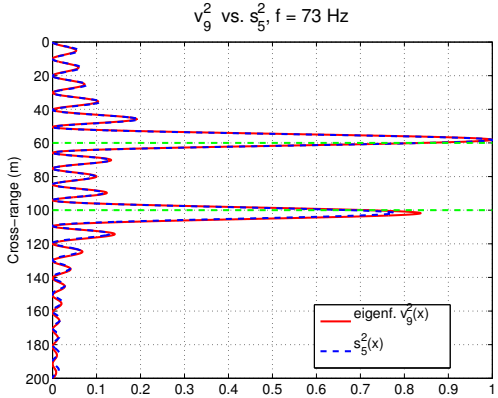

$J = 5$

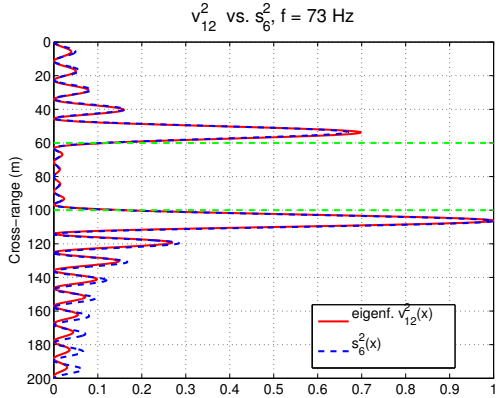

$J = 6$

Selective imaging with $\widetilde{\mathcal{I}}_J^{\mathrm{KM}}$

$f = 73$ Hz, $\alpha = 60$ m and $\beta = 100$ m, $(b = 40$ m$)$.

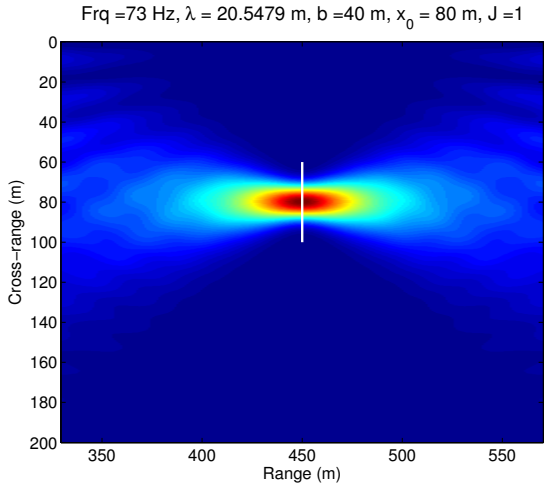

$J = 1$

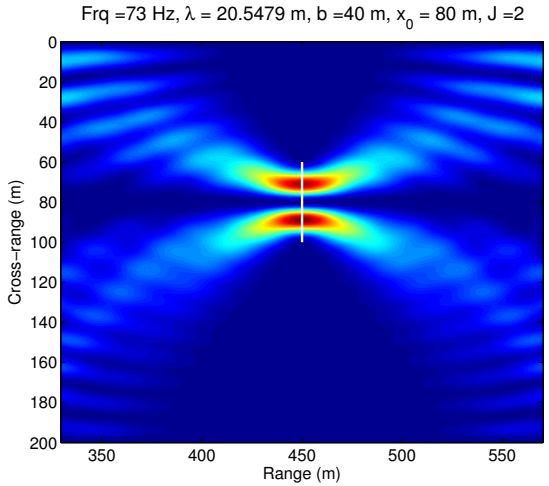

$J = 2$

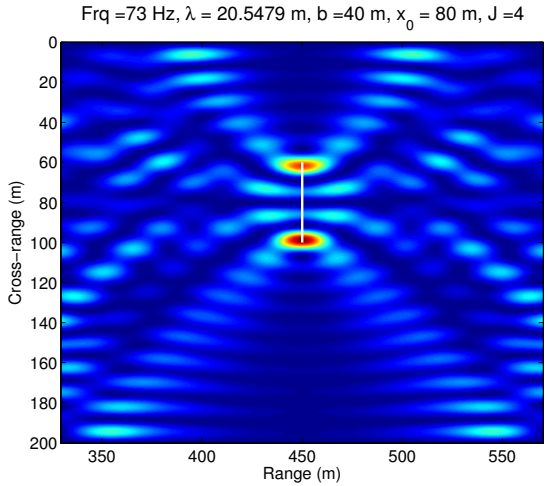

$J = 4$

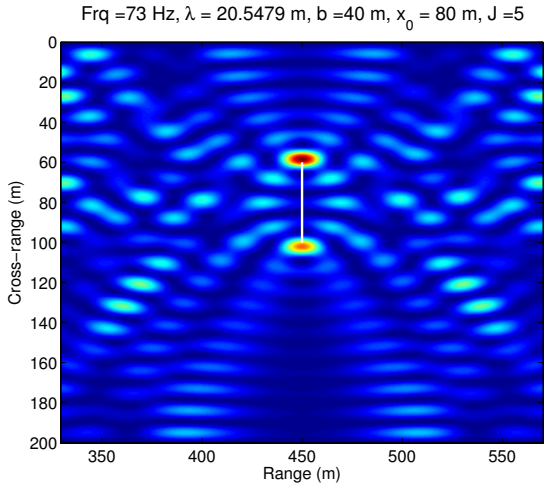

$J = 5$

Table of contents

Modal projection for the partial array

Partial array : $\mathcal{A} \subset [0, D]$.

Main issue : X_n's are no longer orthonormal along $\mathcal{A}$.
Idea : Project on suitable band-limited functions along the array.

In matrix form : Consider

$$S = \begin{pmatrix} \frac{1}{\nu_1} & & & \\ & \frac{1}{\nu_2} & & \\ & & \ddots & \\ & & & \frac{1}{\nu_M} \end{pmatrix} \begin{pmatrix} s_1(x_1) & s_1(x_2) & \dots & s_1(x_N) \\ s_2(x_1) & s_2(x_2) & \dots & s_2(x_N) \\ \vdots & \vdots & \dots & \vdots \\ s_M(x_1) & s_M(x_2) & \dots & s_M(x_N) \end{pmatrix}_{M \times N}$$

where

$$s_J(x_i) = \sum_{k=1}^{M} u_k^J \, X_k(x_i),$$

and $\boldsymbol{u}^J = (u_1^J, u_2^J, \dots, u_M^J)^T$ is the o.n. eigenvector of the Gram matrix $V^T V \rightsquigarrow$ the eigenvalue ν_J.

Recall that

- V is the $N \times M$ matrix with $V_{k\ell} = X_\ell(x_k)$, $k=1,\ldots,N$, $\ell=1,\ldots,M$,
- $D_\beta = \mathrm{diag}(\frac{1}{\beta_1}, \ldots, \frac{1}{\beta_M})$, $\quad Q = \mathrm{diag}(\mathrm{e}^{\mathrm{i}\,\beta_1 L}, \ldots, \mathrm{e}^{\mathrm{i}\,\beta_M L})$ and
- let U be the unitary matrix $U = (\boldsymbol{u}^1, \boldsymbol{u}^2, \ldots, \boldsymbol{u}^M)$.

Recall also that for the crack model problem,

$$\widehat{\Pi} = -\frac{1}{4} V D_\beta Q A_M Q D_\beta V^T.$$

$$\therefore \quad S\,\widehat{\Pi}\,S^T = -\frac{1}{4}\,S\,V\,D_\beta\,Q\,A_M\,Q\,D_\beta\,V^T\,S^T$$

Recall that

- V is the $N \times M$ matrix with $V_{k\ell} = X_\ell(x_k)$, $k=1,\ldots,N$, $\ell=1,\ldots,M$,
- $D_\beta = \mathrm{diag}(\frac{1}{\beta_1}, \ldots, \frac{1}{\beta_M})$, $\quad Q = \mathrm{diag}(\mathrm{e}^{\mathrm{i}\,\beta_1 L}, \ldots, \mathrm{e}^{\mathrm{i}\,\beta_M L})$ and
- let U be the unitary matrix $U = (\boldsymbol{u}^1, \boldsymbol{u}^2, \ldots, \boldsymbol{u}^M)$.

Recall also that for the crack model problem,

$$\widehat{\Pi} = -\frac{1}{4} V D_\beta Q A_M Q D_\beta V^T.$$

$$\therefore \quad S\,\widehat{\Pi}\,S^T = -\frac{1}{4}\,S\,V\,D_\beta\,Q\,A_M\,Q\,D_\beta\,V^T\,S^T$$

But we may prove that

$$SV = U^T \Leftrightarrow USV = I_M$$

Idea : Define the matrix $\hat{\mathbb{P}}$ as

$$\hat{\mathbb{P}} = D_\beta^{-1}\, U\, S\, \hat{\Pi}\, S^T\, U^T\, D_\beta^{-1}.$$

Therefore

$$\begin{aligned}
\hat{\mathbb{P}} &= D_\beta^{-1}\, U\, S\, \hat{\Pi}\, S^T\, U^T\, D_\beta^{-1} \\
&= -\frac{1}{4} D_\beta^{-1}\, \underbrace{U\, S\, V}_{I_M}\, D_\beta Q A_M Q D_\beta\, \underbrace{V^T\, S^T\, U^T}_{I_M}\, D_\beta^{-1} \\
&= -\frac{1}{4} Q A_M Q.
\end{aligned}$$

$\therefore$ $\widehat{\mathbb{P}}$ is unitarily equivalent to A_M.

Idea : Define the matrix $\hat{\mathbb{P}}$ as

$$\hat{\mathbb{P}} = D_\beta^{-1}\, U\, S\, \hat{\Pi}\, S^T\, U^T\, D_\beta^{-1}.$$

Therefore

$$\begin{aligned}
\hat{\mathbb{P}} &= D_\beta^{-1}\, U\, S\, \hat{\Pi}\, S^T\, U^T\, D_\beta^{-1} \\
&= -\frac{1}{4} D_\beta^{-1} \underbrace{U\, S\, V}_{I_M} D_\beta Q A_M Q D_\beta \underbrace{V^T\, S^T\, U^T}_{I_M} D_\beta^{-1} \\
&= -\frac{1}{4} Q A_M Q.
\end{aligned}$$

$\therefore$ $\widehat{\mathbb{P}}$ is unitarily equivalent to A_M.

Note that in the full array case the orthonormality of the X_n's implies : $S = hV^T$ and $U = I_M \Rightarrow US = hV^T$ $\therefore$ we recover the previous definition.

Idea : Define the matrix $\hat{\mathbb{P}}$ as

$$\hat{\mathbb{P}} = D_\beta^{-1}\, U\, S\, \hat{\Pi}\, S^T\, U^T\, D_\beta^{-1}.$$

Therefore

$$\begin{aligned}
\hat{\mathbb{P}} &= D_\beta^{-1}\, U\, S\, \hat{\Pi}\, S^T\, U^T\, D_\beta^{-1} \\
&= -\frac{1}{4} D_\beta^{-1} \underbrace{U\, S\, V}_{I_M} D_\beta Q A_M Q D_\beta \underbrace{V^T\, S^T\, U^T}_{I_M} D_\beta^{-1} \\
&= -\frac{1}{4} Q A_M Q.
\end{aligned}$$

$\therefore$ $\widehat{\mathbb{P}}$ is unitarily equivalent to A_M.

Note that in the full array case the orthonormality of the X_n's implies : $S = hV^T$ and $U = I_M \Rightarrow US = hV^T$ $\therefore$ we recover the previous definition.

N.B. Everything works fine under the assumption that we use exact arithmetic.

In practice : finite precision computations
E.g.

$$S = \mathrm{diag}\Big\{ \frac{1}{\nu_1}, \ldots, \frac{1}{\nu_M} \Big\} \Big(s_i(x_j) \Big)_{i=1,\ldots,M, j=1,\ldots,N}$$

where ν_i are the eigenvalues of $V^T V$.

Note that $V^T V$ may be viewed as an approximation of the $M \times M$ matrix A_{arr} with

$$(A_{\mathrm{arr}})_{mn} = \frac{1}{h} \int_{\mathcal{A}} X_n(x) X_m(x) dx, \ m, n = 1, 2, \ldots, M.$$

A_{arr} is a Toeplitz-minus-Hankel matrix.

Let l_{arr} is the array length. Then

- approx. $[l_{\mathrm{arr}}/(\lambda/2)]$ are close to 1, and
- $M - [l_{\mathrm{arr}}/(\lambda/2)]$ approach 0.

Therefore as l_{arr} decreases more singular values tend to zero, and in fact $V^T V$ will become practically singular as soon as its minimum singular value $\mu_{\min}$ falls below some threshold.

Behavior of the minimum s.v. of $V^T V$

The length of the array is decreased symmetrically

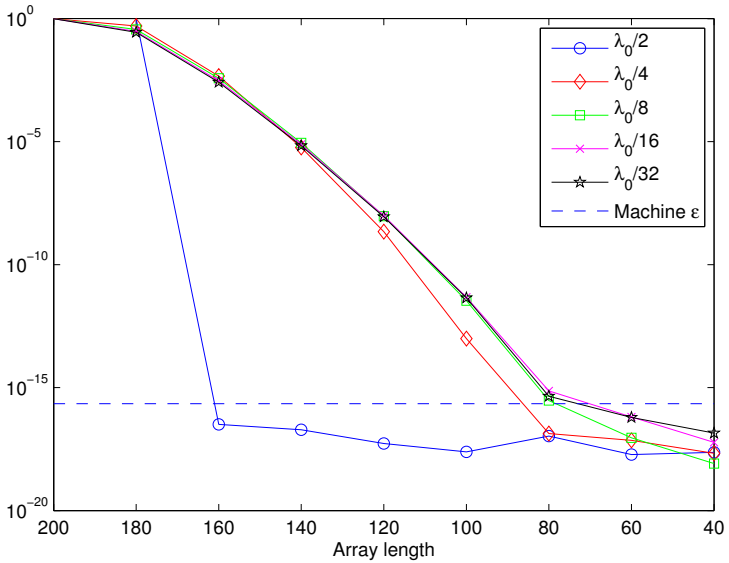

Table of contents

Crack : Imaging with $\widetilde{\mathcal{I}}^{\mathrm{KM}}$ and $\mathcal{I}^{\mathrm{KM}}$

$D = 200$ m, $c_0 = 1500$ m/s, $f = 73$ Hz, (for $f_0 = 75$ Hz, $\lambda_0 = 20$ m),
$h = \lambda_0/8 = 2.5$ m. Crack : length $b = 40$ m, center : $(450, 100)$ m.

$\widetilde{\mathcal{I}}^{\mathrm{KM}}$

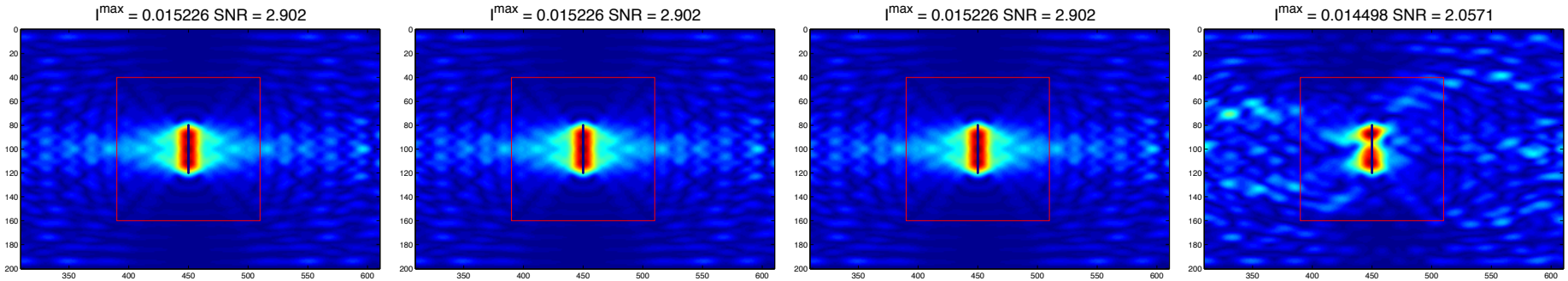

$\mathcal{I}^{\mathrm{KM}}$

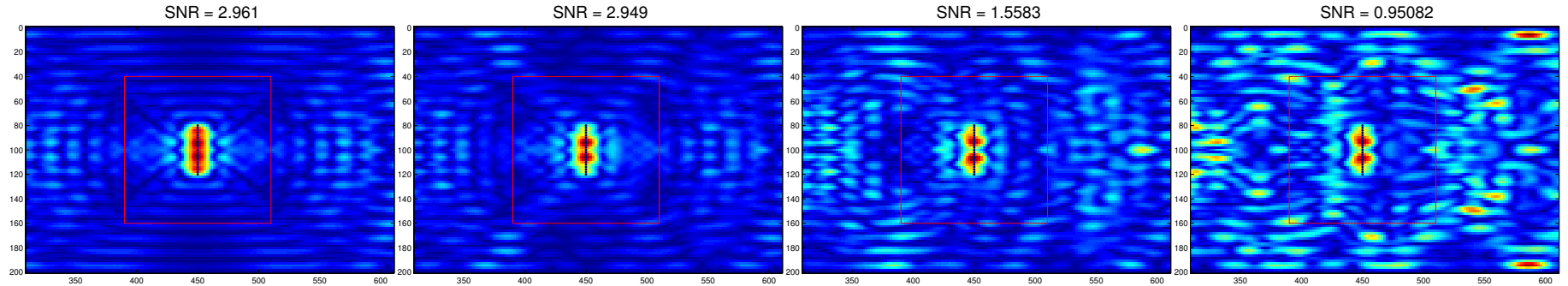

$|\mathcal{A}| = 200$ m $\quad |\mathcal{A}| = 180$ m $\quad |\mathcal{A}| = 140$ m $\quad |\mathcal{A}| = 80$ m

Crack : Selective imaging with $\widetilde{\mathcal{I}}_J^{\mathrm{KM}}$

$|\mathcal{A}| = 180$ m (90% of the total depth) (array is cut symmetrically)

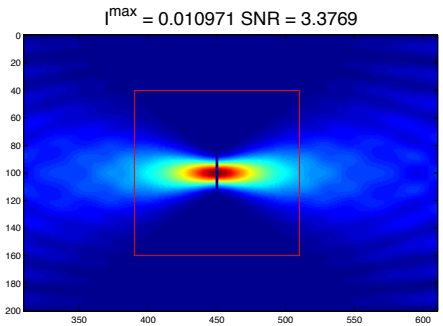

$J = 1$

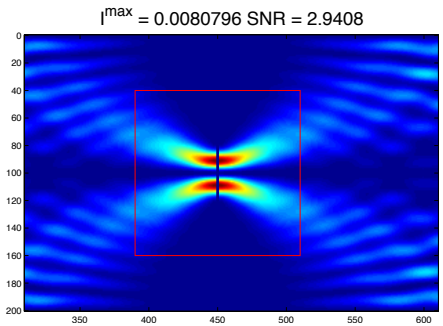

$J = 2$

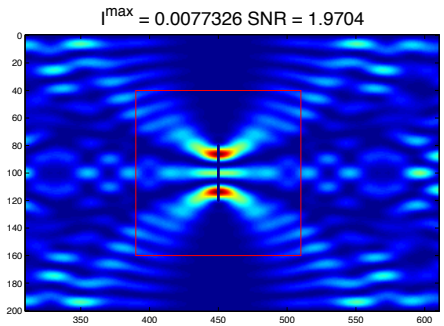

$J = 3$

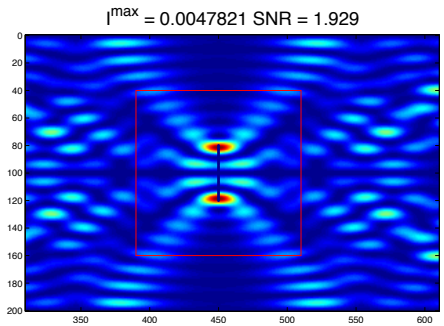

$J = 4$

Crack : Imaging with $\widetilde{\mathcal{I}}^{\mathrm{KM}}$ and selective imaging with $\widetilde{\mathcal{I}}_J^{\mathrm{KM}}$

$|\mathcal{A}| = 60$ m (30% of the total depth) (array is cut symmetrically)

$\widetilde{\mathcal{I}}^{\mathrm{KM}}$

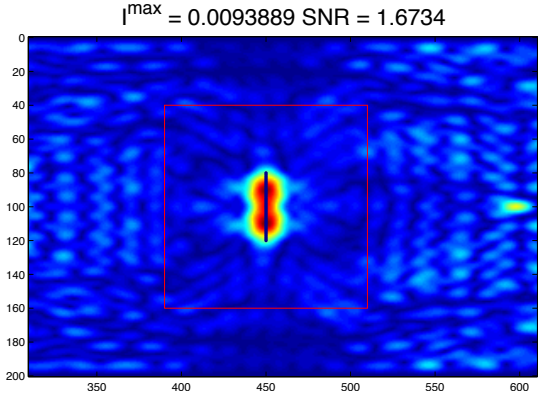

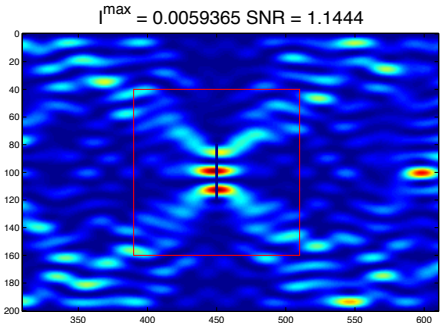

$J = 1$

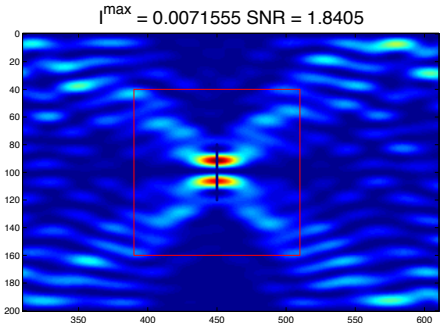

$J = 2$

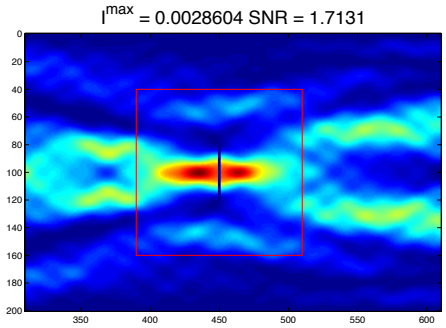

$J = 3$

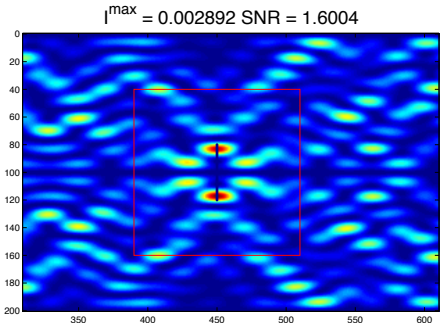

$J = 4$

Square : Imaging with $\widetilde{\mathcal{I}}^{\mathrm{KM}}$ and selective imaging with $\widetilde{\mathcal{I}}_J^{\mathrm{KM}}$

$|\mathcal{A}| = 180$ m (90% of the total depth) (array is cut symmetrically)

$\widetilde{\mathcal{I}}^{\mathrm{KM}}$

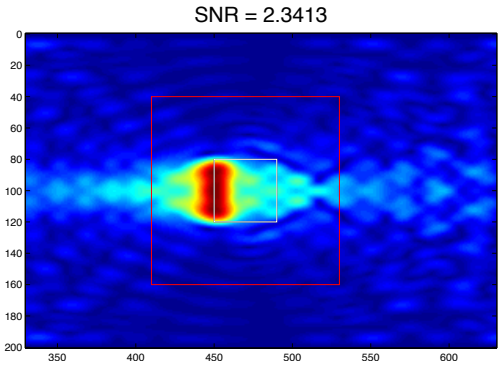

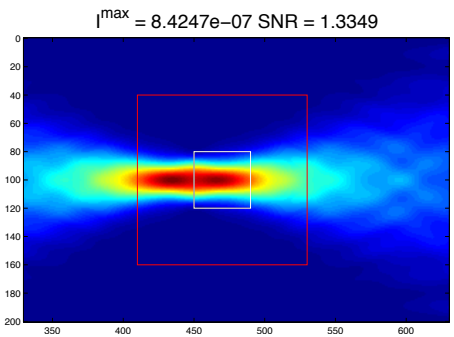

$J = 1$

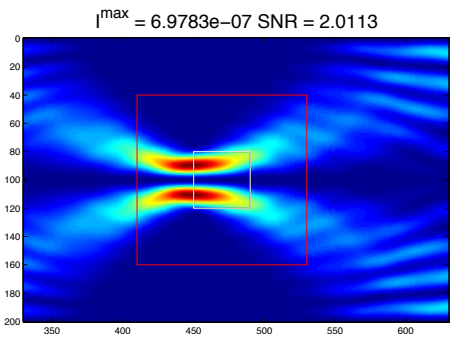

$J = 2$

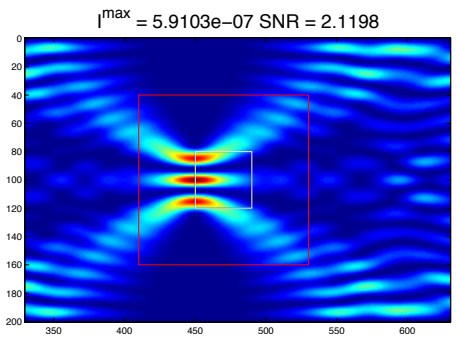

$J = 3$

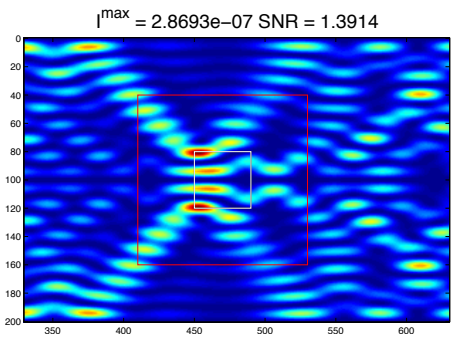

$J = 4$

Square : Imaging with $\widetilde{\mathcal{I}}^{\mathrm{KM}}$ and selective imaging with $\widetilde{\mathcal{I}}_J^{\mathrm{KM}}$

$|\mathcal{A}| = 140$ m (70% of the total depth) (array is cut symmetrically)

$\widetilde{\mathcal{I}}^{\mathrm{KM}}$

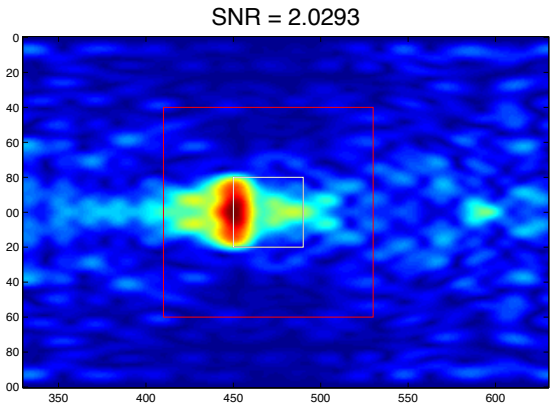

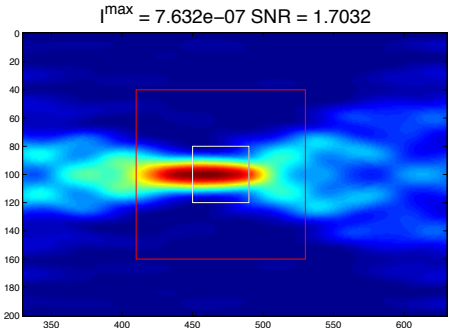

$J = 1$

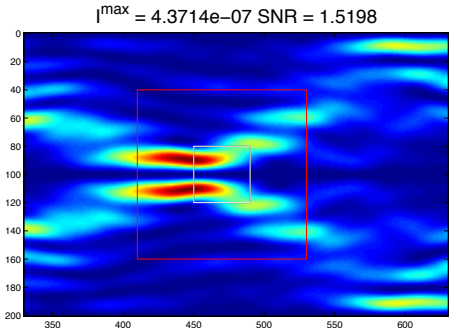

$J = 2$

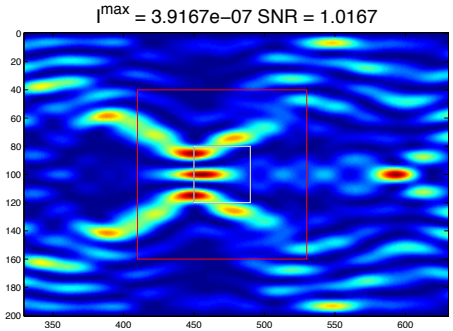

$J = 3$

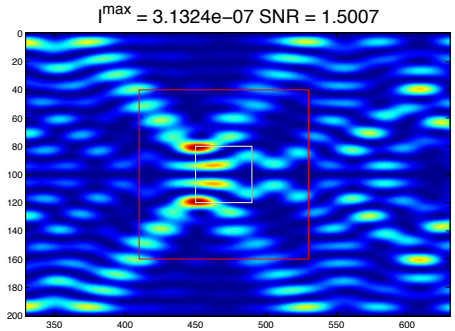

$J = 4$

Square : Imaging with $\widetilde{\mathcal{I}}^{\mathrm{KM}}$ and selective imaging with $\widetilde{\mathcal{I}}_J^{\mathrm{KM}}$

$|\mathcal{A}| = 120$ m (60% of the total depth) (array is cut symmetrically)

$\widetilde{\mathcal{I}}^{\mathrm{KM}}$

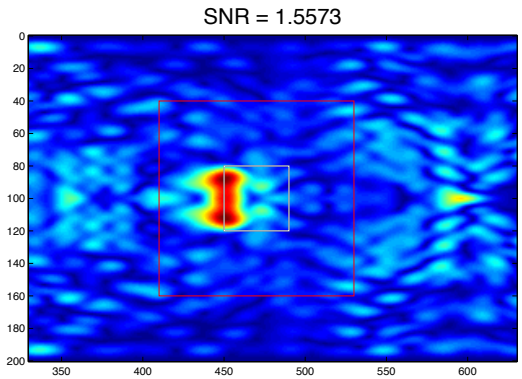

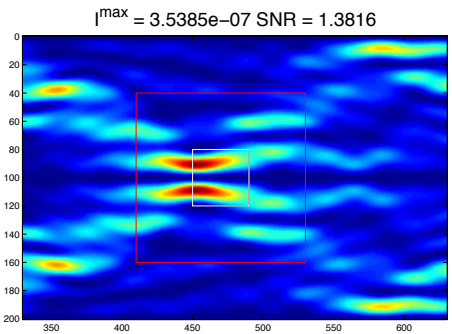

$J = 1$

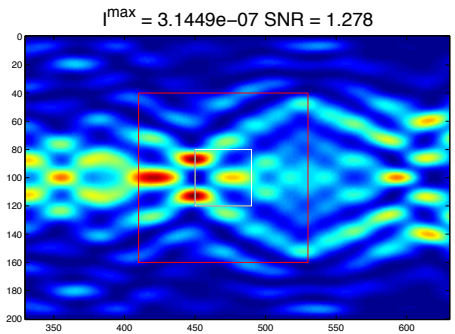

$J = 2$

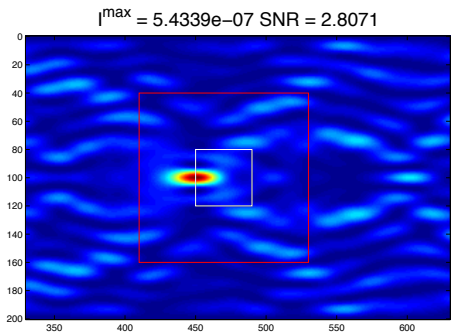

$J = 3$

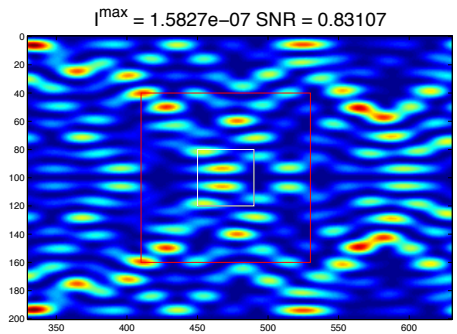

$J = 4$

Table of contents

Conclusions/Future Work

Conclusions

- We have proposed a new selective imaging functional based on Kirchhoff migration and the s.v.d. of $\widehat{\mathbb{P}}(\omega)$, which is a weighted modal projection of the array response matrix.
- For a model problem ('crack') : $\operatorname{rank}\left(\hat{\mathbb{P}}(\omega)\right) \approx \left[\frac{b}{\lambda/2}\right]$.
- For the model problem, we fully characterised the singular vectors of $\hat{\mathbb{P}}(\omega)$ and the imaging functional along the crack.
- We extended our methodology to the partial aperture case using a projection on suitable band-limited functions along the array.

C.T., D. A. Mitsoudis and S. Papadimitropoulos, Selective imaging of extended reflectors in two-dimensional waveguides, SIAM Journal on Imaging Science, Vol. 6, No. 4, pp. 2714–2739, 2013.
C.T., D. A. Mitsoudis and S. Papadimitropoulos, Partial aperture imaging in acoustic waveguides, preprint

Work in progress

- inhomogeneous medium,
- multiple extended scatterers.

Conclusions/Future Work

Conclusions

- We have proposed a new selective imaging functional based on Kirchhoff migration and the s.v.d. of $\widehat{\mathbb{P}}(\omega)$, which is a weighted modal projection of the array response matrix.
- For a model problem ('crack') : $\operatorname{rank}\left(\hat{\mathbb{P}}(\omega)\right) \approx \left[\frac{b}{\lambda/2}\right]$.
- For the model problem, we fully characterised the singular vectors of $\hat{\mathbb{P}}(\omega)$ and the imaging functional along the crack.
- We extended our methodology to the partial aperture case using a projection on suitable band-limited functions along the array.

C.T., D. A. Mitsoudis and S. Papadimitropoulos, Selective imaging of extended reflectors in two-dimensional waveguides, SIAM Journal on Imaging Science, Vol. 6, No. 4, pp. 2714–2739, 2013.
C.T., D. A. Mitsoudis and S. Papadimitropoulos, Partial aperture imaging in acoustic waveguides, preprint

Work in progress

- inhomogeneous medium,
- multiple extended scatterers.

Thank you !